Chapter 2

MATHEMATICAL MODELING IN NUTRITION: CONSTRUCTING A PHYSIOLOGIC COMPARTMENTAL MODEL OF THE DYNAMICS OF β-CAROTENE METABOLISM

JANET A. NOVOTNY

Diet and Human Performance Laboratory
Beltsville Human Nutrition Research Center
U. S. Department of Agriculture
Beltsville, Maryland 20705

LOREN A. ZECH

Laboratory of Mathematical Biology, National Cancer Institute
Bethesda, Maryland 20892

HAROLD C. FURR

Department of Nutritional Sciences, University of Connecticut
Storrs, Connecticut 06269

STEPHEN R. DUEKER AND ANDREW J. CLIFFORD[1]

Department of Nutrition, University of California
Davis, California 95616

[1] Corresponding author.

I. INTRODUCTION AND BACKGROUND

To understand the health implication of current and recommended dietary practices, i.e., increased intakes of some foods and/or nutrients such as fruits and vegetables and antioxidant vitamins and reduced intakes of others such as calories and saturated fats, an investigation of variations in health status produced by these practices is required. Tracer studies are often used to characterize the health status of individuals because their response patterns are consistent and such studies can be interpreted in a standardized way. Tracer kinetics are usually modeled with differential equations that are mapped to metabolic spaces and the exchanges (analyte flows) between them in the domain of an individual's (a system's) metabolism. The characteristics of these spaces and the exchanges (of nutrients/analytes) that take place between them provide much useful information about an individual's physiologic status. Computer hardware and modeling software capable of solving (and manipulating) differential equations efficiently and accurately are now available. Therefore, mathematical modeling has become an attractive tool for collecting and processing the research data and information needed to discover those optimal combinations of nutrients that promote health and prevent and/or minimize disease.

While many researchers have focused on the tools of molecular biology and genetics to determine biochemical mechanisms of nutrient action in animal models, a few have focused on mathematical modeling of kinetic data to achieve a quantitative understanding of the dynamics of nutrient metabolism *in vivo* (for recent symposia, see Abumrad, 1991; Coburn, 1992). Three recent developments stimulated interest in mathematical modeling. First, there is an opportunity to integrate quantitative characteristics of the dynamics of nutrient metabolism with knowledge of nutrient action mechanisms and health status. Second, it appears that some animal models do not mimic nutrient metabolism and health status of humans. Third, stable isotope tracers and reliable methods to measure minute amounts of them in human tissues have become more readily available.

Stable isotopes are advantageous both because there is no radiation exposure to study subjects and the problems of disposing of radionuclides are avoided. The combined use of such tools as mathematical models and stable isotopes is a powerful approach for understanding the dynamics of nutrient metabolism and for tailoring their requirements to physiologic state and age.

Compartmental modeling has been successfully employed to gain new integrated and quantitative insights into several biological and physical systems currently under investigation. Compartmental modeling papers have generally only detailed the theoretical basis for modeling and then

summarized the final results of their studies; details concerning model development usually have been omitted. Because the rationale, philosophy, and details for developing a compartmental model are not well described in the scientific literature, some investigators have limited their approach to empirical descriptions of their research data. Consequently they have been unable to maximize the information potentially obtainable from their studies. This paper aims to describe the practical aspects of the process of developing a physiologically based compartmental model using a recently constructed model of the dynamics of β-carotene metabolism. Also, we discuss how compartmental modeling itself has advanced understanding of β-carotene and retinol metabolism.

The reason for building a physiologic compartmental model is to realize as complete a description as possible of a metabolic system under investigation. The model is built to develop an analogy of the system under investigation and to obtain values for critical parameters of the model so that unobserved portions of the dynamic and kinetic behavior of the system under investigation can be predicted. Specific information obtained about the system under investigation includes the number of pools and their sizes, how they are connected, and how their masses change over time.

Physiologic compartmental models are built by analogy with a specific physiologic system under investigation in order to rigorously describe assumptions about the system and to subsequently test these assumptions. This is often accomplished by a comparison of a plasma analyte concentration–time curve predicted by the model to the actual experimental observations. Physiologic compartmental models are chosen because they can be assumed to be a suitable analogy to the physiologic system under investigation which, in turn, is assumed to consist of pools and flows of analytes. On the other hand, empirical descriptions of the system under investigation have limited use because they are less able to describe complex metabolic relationships. Therefore, by building a compartmental model of the system under investigation, it is possible to gain a greater understanding of the system, to extract considerably more information about it from the experimental observations, and to identify gaps in the existing knowledge of the system. Relationships among the system under investigation, the model, and the experimental observations are depicted in Fig. 1.

The goal of the modeling process is the full realization of the system under investigation by relating elements of the model with the experimental observations. Model structure specification (connectivity) and identification (defining model parameters and estimating numerical values for them and their precision from the noisy data) are mapped to the system's metabolic spaces and the transfer of analyte among them. The system under investigation is fully understood or realized by an analogy (point by point compari-

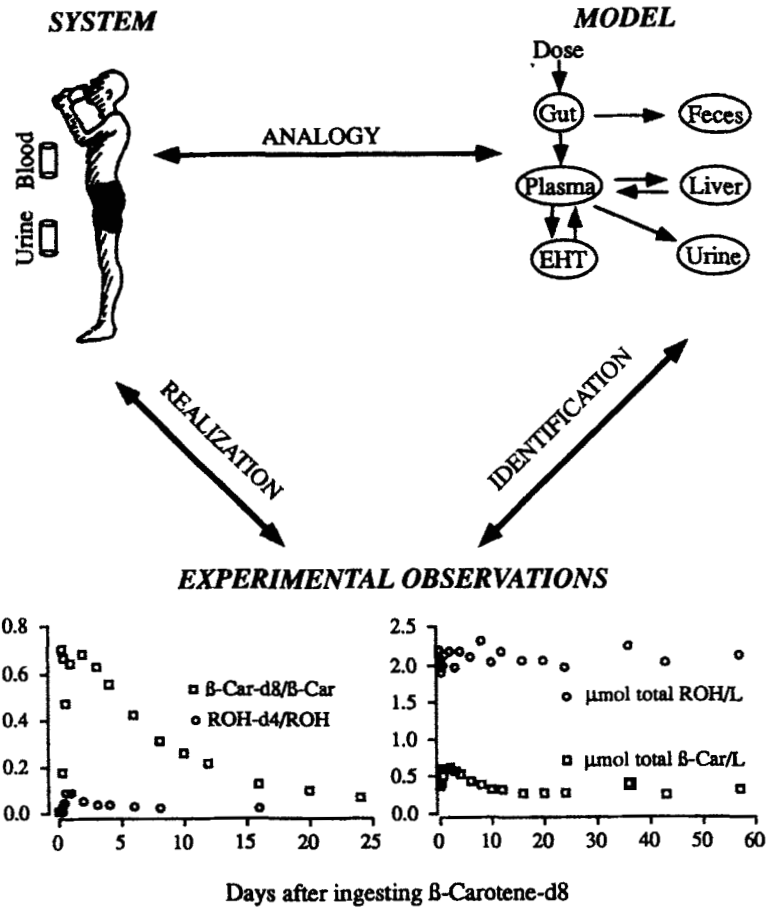

FIG. 1. Relationships among the model, the system under investigation and the experimental observations. EHT = extrahepatic tissue; ROH = retinol; β-Car = β-Carotene. Isotopomer ratios of β-carotene-d_8/β-carotene and retinol-d_4/retinol and the concentrations of total β-carotene and total retinol in plasma by time since ingesting β-carotene-d_8 (the experimental measurements) are shown in the bottom left and right panels, respectively. Rudiments of the model include the compartment; the fractional transfer coefficient and flow from a donor to a recipient compartment; the initial conditions of the system; and a set of rules for relating elements of the model with the experimental observations made on the system under investigation.

son) of the experimental observations with the model's predicted curve; this comparison is called the fit. Building a model can facilitate the realization of a system under investigation because the model is an analogy of that system. Thus, by identification and analogy, model building allows the system under investigation to be realized and evaluated by how well the model predicts the experimental observations.

Practical aspects of the process of developing a physiologic compartmental model are illustrated using a recently constructed model of the dynamics of β-carotene metabolism (Novotny *et al.*, 1995). β-Carotene is not only a significant source of vitamin A for humans worldwide, but is also reported to protect against oxidative stress, heart disease, and cancer and to enhance the immune response (Krinsky, 1989; Olson, 1992; Bendich, 1993). β-Carotene is used in large amounts both as a dietary supplement and in many clinical trials. However, despite its key physiologic effects and widespread intake, the dynamics of the metabolism of this common diet constituent in humans as well as the factors that affect it are largely unknown. This encouraged us to build a physiologic compartmental model of the dynamics of β-carotene metabolism in a healthy adult *in vivo*.

II. MATERIALS, METHODS, AND MODEL CONSTRAINTS

An informed, consenting, and healthy 53-year-old male, weighing 94 kg, ingested a gelatin capsule containing 73 μmol (40 mg) of all-*trans*-β-carotene-10,10′,19,19,19,19′,19′,19′-d_8 (β-carotene-d_8) dispersed in ~2g olive oil. This material was synthesized and its chemical and isotopic purities were determined as previously described (Bergen, 1992; Dueker *et al.*, 1994). The capsule was ingested with a light breakfast, and the subject ate a lunch and dinner at 3 and 8 hr later, respectively, that were very low in carotene and vitamin A. Blood samples were drawn just before (0 hr) and at 0.5, 1, 2, 5, 7, 9, 12, and 24 hr and 2, 3, 4, 6, 8, 10, 12, 16, 20, 24, 36, 43, 57, 71, 85, 99, and 113 days after ingestion of the β-carotene-d_8 containing capsule. Only data for the first 57 days are used, because the tracer concentrations were too low to analyze accurately after that point. The protocol was approved by the University of California, Davis, Human Subjects Review Committee.

Plasma was separated by centrifugation and the concentrations of total (deuterated and protonated) β-carotene and total retinol in all plasma specimens (after saponification) were measured by high-performance liquid chromatography (HPLC); the fractional standard deviation (FSD) of the analytical method was <0.04. Ratios of β-carotene-d_8/β-carotene in all plasma specimens were determined by HPLC; the FSD of this analytical method was 0.0325. Ratios of retinol-d_4/retinol in all plasma specimens were determined by gas chromatography mass spectrometry; the FSD of this method was 0.045. Details of these laboratory analytical procedures are previously described (Handelman *et al.*, 1993; Dueker *et al.*, 1993, 1994). The physiologic compartmental model of the dynamics of β-carotene metabolism based on these data is also previously described (Novotny *et al.*,

1995). Plasma isotopomer ratios and concentrations of plasma total β-carotene and total retinol by time since ingesting β-carotene-d_8 (the experimental measurements) are shown in the bottom of Fig. 1.

To allow plotting of the concentration–time data for the tracer, the ratio of β-carotene-d_8/β-carotene in each plasma specimen was multiplied by the concentration of total β-carotene in that specimen to obtain the concentration of β-carotene-d_8 in each specimen. The concentration of retinol-d_4 in each plasma specimen was calculated as the ratio of retinol-d_4/retinol times the concentration of total retinol. So that compartmental modeling could be performed using units of analyte mass in the plasma compartment (for example), the concentrations of total β-carotene and total retinol in plasma were multiplied by the subject's estimated plasma volume to give the total mass of β-carotene and retinol in the plasma compartment. The 94-kg test subject was assumed to have 45 ml plasma/kg body wt (Snyder *et al.*, 1975), and the estimated plasma volume therefore was 4.23 liters.

Our knowledge of the system in steady state consisted of the β-carotene status of the test subject (as estimated from plasma) and information gathered from the scientific literature. Since β-carotene concentrations in tissues (other than plasma) of the test subject were not measured directly, model tissue β-carotene reserves in steady state were statistically constrained to those values reported in other studies from the scientific literature. The total reserves of β-carotene in hepatic and extrahepatic tissues were constrained to be 6.73 ± 1.34 and 9.5 ± 1.90 μmol (mean ± 2 SD), respectively, based on HPLC-measured concentrations of β-carotene in human tissues (Schmitz *et al.*, 1991, 1993; Zulim *et al.*, 1995) times the masses of the tissues of the ICRP No. 23 reference man (Snyder *et al.*, 1975).

The stoichiometry of conversion of β-carotene to retinol is still an unsettled issue. Central cleavage of β-carotene theoretically yields 2 mol retinol per mole β-carotene (Goodman and Huang, 1965; Olson and Hayaishi, 1965; Olson, 1989) and eccentric cleavage of β-carotene yields 1 mol retinol per mole β-carotene (Olson, 1989, Krinsky *et al.*, 1994). Brubacher and Weiser (1985) determined the retinol equivalent of β-carotene *in vivo* using rats and chicks and found that 1 mol of absorbed β-carotene yielded 1 mol retinol. Because the body reserves of retinol in these animals were low, the yield of retinol from β-carotene was probably maximal. Based on these *in vivo* results, a ratio of 1 mol retinol per mole β-carotene (after absorption) was used in constructing the present compartmental model of the dynamics of β-carotene metabolism.

Normally in tracer studies, the size (mass) of the tracer dose is carefully chosen to be only a fraction of the mass of the tracee in the system under investigation so that the steady-state metabolism of the tracee is unaffected. However, in the present study a rather large dose of β-carotene-d_8 was

administered (73 μmol or ~10 times the usual daily intake of β-carotene) to insure that the tracer and its labeled metabolite (retinoid-d_4) could be measured reliably in plasma because only ~15% of the dose was expected to be absorbed (Bowen *et al.*, 1993). Also, the 73-μmol dose was intermediate between a usual daily intake and the doses used in many clinical trials and was therefore physiologically relevant.

In developing the compartmental model of the dynamics of β-carotene metabolism, the behavior of the system under investigation was viewed from three different vantage points by considering the tracer in the system, the tracee in the system, and the undisturbed (steady-state) system. First, the tracer was considered by following the rise and fall in the plasma concentration of β-carotene-d_8 and retinol-d_4 by time after ingestion of the β-carotene-d_8. Second, the tracee was considered in the presence of the tracer by measuring the plasma total β-carotene and total retinol concentrations by time after ingestion of the β-carotene-d_8. Third, the steady state of the system under investigation was considered by including the baseline plasma β-carotene concentration, the baseline plasma retinol concentration, and the masses of liver and extrahepatic tissue β-carotene as estimated from recently published data. Information from all three vantage points was included in the model and solved simultaneously to determine the behavior of the system.

We began modeling under the assumption that the introduction of the tracer (mass) into the system did not affect the mechanisms present for metabolism of the tracee. The compartmental model was compatible with the assumption that non-steady-state mechanisms for metabolism of β-carotene were not induced by the tracer because the model prediction of the tracer state, the tracee state, and the steady state could be achieved using the same set of fractional transfer coefficients (FTCs). The appropriateness of this assumption is discussed again under Statistical Considerations. FTC is the fraction of analyte in a donor compartment that is transferred to a recipient compartment per unit of time, in this case per day.

Compartmental modeling was performed using SAAM 31 software[2] (Berman and Weiss, 1978) on a Dell 466/T as described by Novotny *et al.*, (1995). The SAAM software was chosen because it was developed specifically, but not exclusively, for the study of mathematical models expressed in the context of a group of connected compartments. SAAM was developed by modelers, it is equipped with many features which are especially useful for modeling, it allows the model to be stated in terms of physiologic pools

[2] This SAAM 31 software is available at no cost from Dr. Loren Zech, NCI, Building 10, Room 6B-13, Bethesda, MD 20892. Internet address greif@saam.nci.nih.gov. This software can also be obtained via modem at (301) 480-3295 (login as zmodem) or via anonymous ftp: ftp@saam.nci.nih.gov.

and flows, and it has been successfully used for modeling for several decades. An interface called CONSAM is available so that models may be altered and evaluated interactively rather than only in batch mode. This facilitates the modeling by making the computing faster and easier.

III. THE PROCESS OF CONSTRUCTING A COMPARTMENTAL MODEL

The first step in constructing a compartmental model is to examine the experimental observations for clues concerning the functionality of the system. This is especially true if the experimental observations are available prior to modeling because it helps direct the construction of the model. The experimental observations were available when construction of the compartmental model of the dynamics of β-carotene metabolism started.

The model was developed by adjusting the connectivity of the model to improve the fit and the model was modified until it provided an adequate fit of the experimental observations. Therefore, the model is accepted as an hypothesis of the dynamics of β-carotene metabolism to be tested.

Construction of the physiologic compartmental model began with a simple conceptual model based on existing knowledge of β-carotene and retinol metabolism. The simplest version of a relevant compartmental model is depicted in Fig. 2.

In this conceptual model, a single oral dose of β-carotene passes through a stomach compartment and enters an intestine compartment, where it is prepared for absorption. During absorption, intact β-carotene is absorbed and transferred to a plasma chylomicron (which become remnants by removal of triglycerides) compartment from where it transfers to a liver compartment and is rereleased into a plasma lipoprotein compartment (Krinsky *et al.*, 1958; Cornwell *et al.*, 1962; Clevidence and Bieri, 1993) for delivery to an extrahepatic compartment. Eventually β-carotene metabolites are lost irreversibly from the extrahepatic tissue compartment (EHT) into plasma and returned to liver for disposal probably via bile or other irreversible loss. Since plasma lipoproteins are taken up by liver (Langer *et al.*, 1972), β-carotene in the lipoprotein compartment would be recycled back to liver, even several times; this pathway is included in the model.

During absorption some β-carotene is also converted to retinoid (Dimitrov *et al.*, 1988; Olson, 1989; van Vliet *et al.*, 1992; Scita *et al.*, 1993) and transferred via a plasma chylomicron (remnant) retinyl ester compartment to a liver retinyl ester compartment. From here it is released in a plasma retinol-binding protein–retinol (RBP-ROH) compartment for transfer to target tissues. Eventually it is lost irreversibly from the RBP-ROH compart-

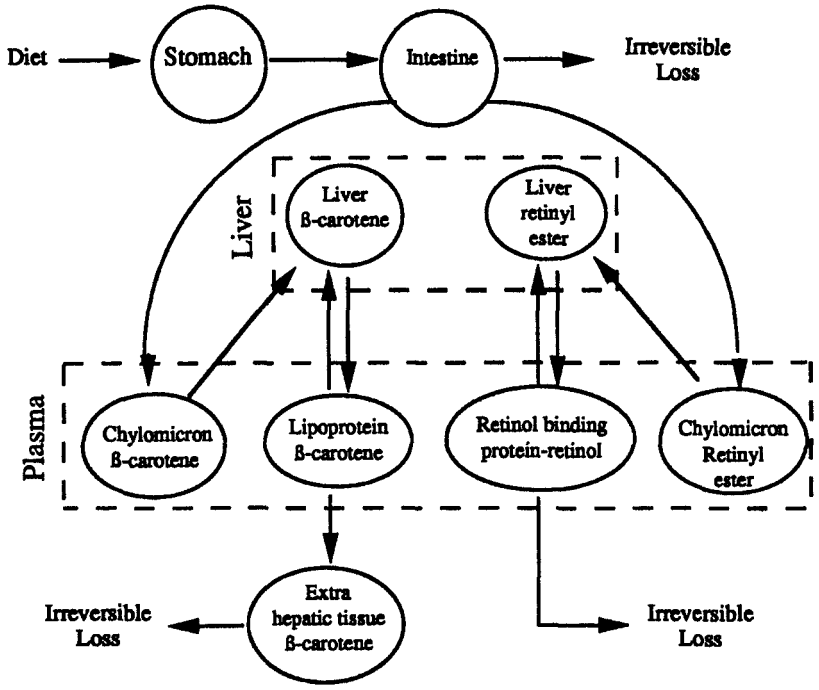

FIG. 2. Conceptual physiologic compartmental model of β-carotene metabolism in humans. Each circle represents a kinetically distinct form of β-carotene or retinoid. The arrows indicate flows between compartments. Reprinted with permission from Novotny et al. (1995).

ment partly through the kidneys. Since plasma retinol can also be recycled from plasma back to liver several times (Green and Green, 1994), a path to transfer retinol from the RBP-ROH compartment back to the liver retinyl ester compartment is included. Finally, it is assumed that conversion of β-carotene to retinoid occurred only at the level of the intestine; i.e., significant conversion did not occur in liver even though the carotenoid-15,15′-dioxygenase enzyme that catalyzes the conversion occurs there.

Thus the conceptual structure of the model has been established. At this point, the numerical values (and their precision from the noisy data) for the model parameters must then be determined. Approximate values for the parameters (FTCs, flow rates, etc.) may be determined in several ways. One can search the scientific literature for turnover rates of the relevant and/or related analytes, extrapolate values from experimentally measured kinetic data for the relevant analytes, and/or reason to a set of values based on available knowledge of the system under investigation. Once

approximate values for the parameters are established, they are combined with the conceptual structure of the model to simulate the behavior of the system. The strength of the model in predicting the experimental observations (in this case, the concentrations of β-carotene-d_8, retinoid-d_4, total β-carotene, and total retinol in plasma) is then investigated. Any discrepancies between the compartmental model's prediction of the system's behavior and the experimental observations are further used to direct physiologically meaningful alterations to the model's structure specification, parameter identification, and estimation. The system under investigation is realized or explained when all discrepancies have been minimized.

Model parameters can be defined as one or a set of measurable factors that define a system under investigation, determine its behavior, and are varied in an experiment. Model parameters can also be defined as a quantity or constant in an equation whose value varies in other equations of the same general form. After each alteration to the model parameters, the differential equations that describe the model are solved (or manipulated) and the ability of the model to predict the experimental observations is again investigated. The process of altering (refining) the model, solving and/or manipulating the differential equations, and evaluating the predictive behavior of the model may undergo many iterations in developing a good compartmental model of a complex metabolic system. In developing the compartmental model of the dynamics of β-carotene metabolism, for example, the model-generated curves of β-carotene-d_8, retinol-d_4, total β-carotene, and total retinol concentrations in plasma were simultaneously compared repeatedly with the experimentally measured (observed) concentrations.

In addition to considering the plasma concentrations of β-carotene-d_8, retinol-d_4, total β-carotene, and total retinol in fitting the model-predicted line for each of those quantities to the experimental observations, various other metabolic quantities were also predicted to insure that the model predicted the system's behavior in a physiologically reasonable manner. For example, the predicted daily intake of β-carotene was compared to knowledge of normal daily β-carotene intake by adults, and the predicted liver reserves of retinol (ester) were compared to those reported in other studies. The discrepancies between the model prediction and the experimental observations were again used to plan more alterations to the model to improve its fit with the system's behavior. Some alterations to the model are bound to compromise rather than improve the model's prediction of the system's behavior. Never the less, with each alteration to the model, something new is still discovered about the system and a more complete understanding of it, as discussed later in Fig. 3, results. These are the rewards of compartmental modeling.

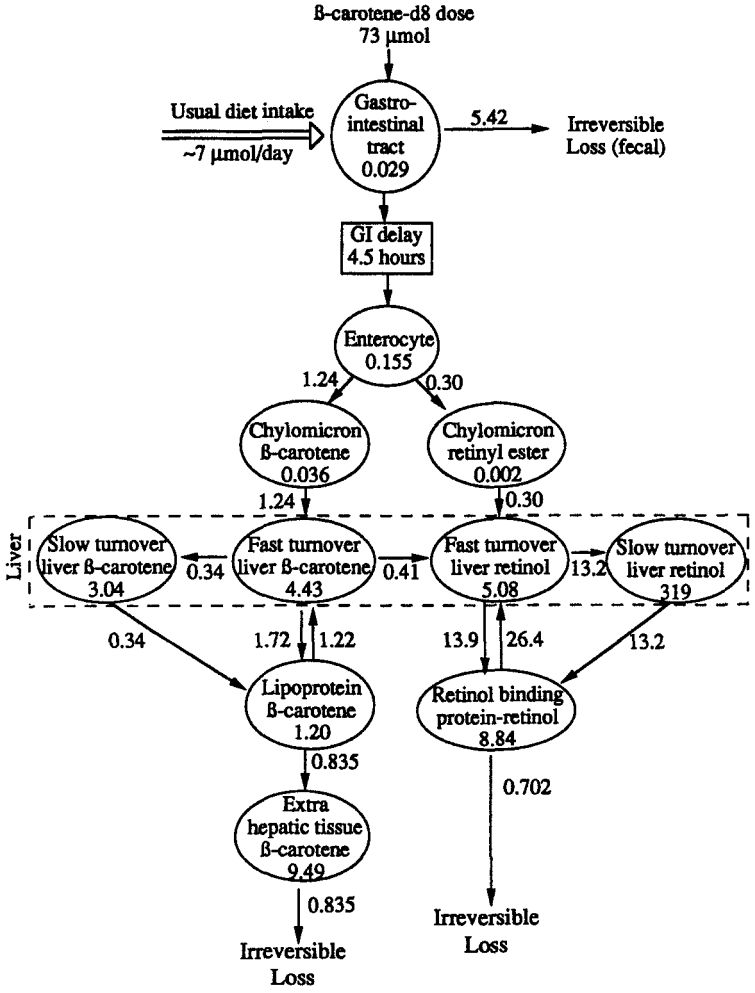

FIG. 3. Physiologic compartmental model of the dynamics of β-carotene metabolism in an adult volunteer. Each circle represents a kinetically distinct form of β-carotene or retinoid. The rectangle represents a delay element. For each compartment, the compartmental model predicted the total mass (reserves) of β-carotene or retinoid in each compartment at steady-state; they appear as μmol in each circle/oval. Values by the arrows are flow rates among compartments in μmol/day. Reprinted with permission from Novotny *et al.* (1995).

IV. INTERMEDIATE MODELS

Each alteration to the model parameters and associated iteration leads to the creation of a new (intermediate) model and a new prediction of

the system's behavior. The following section describes some of the major alterations made to the conceptual structure of our example model, as well as the numerical values for the model parameters, the key observations that prompted the changes, and how these changes improved the model prediction.

Neither β-carotene-d_8 nor retinol-d_4 were detected in plasma until 5 hr after the β-carotene-d_8 was ingested (see expanded insets in left panels of Fig. 4). Therefore, a gastrointestinal (GI) delay compartment of 4.5 hr and an enterocyte compartment were added to the model. The delay represents the time necessary for β-carotene-d_8 (taken with the breakfast) to pass through the gastrointestinal tract and form lipid micelles in preparation for absorption by the enterocyte. Reducing the FTC from the GI delay compartment to the plasma β-carotene compartment was not an effective way to represent the delay because it flattened the first slope (rise) of the plasma β-carotene-d_8 concentration–time curve, whereas adding the

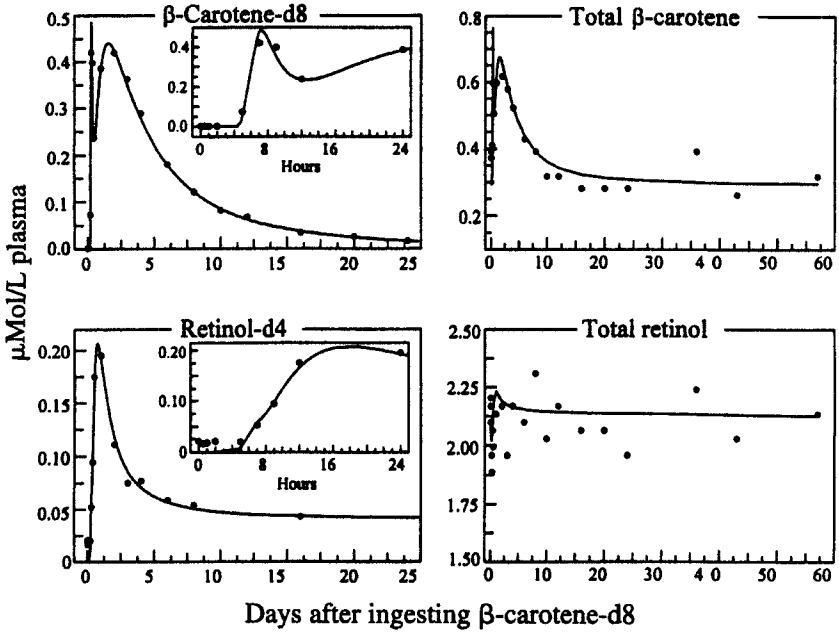

FIG. 4. Experimentally measured values (circles) and the best-fit line using the physiologic model of the plasma concentrations of β-carotene-d_8 (top left), of retinol-d_4 derived from ingested β-carotene-d_8 (bottom left), of total β-carotene, labeled plus nonlabeled (top right), and of total retinol, labeled plus nonlabeled (bottom right). Reprinted with permission from Novotny *et al.* (1995).

GI delay compartment provided the necessary delay and allowed a steeper rise in the β-carotene-d_8 concentration–time curve.

Once the delay and enterocyte compartments were added, the initial slope (rise) in the plasma β-carotene-d_8 concentration–time curve was still shallower than the rise observed with the experimental observations. Reasoning that the initial sharp rise in the plasma β-carotene-d_8 data represented chylomicron β-carotene rapidly entering the plasma, we increased the FTC of β-carotene from the enterocyte compartment to the plasma chylomicron compartment until the initial slope (rise) in the model-predicted plasma β-carotene-d_8 concentration–time curve matched the rise that occurred in the experimental observations as shown in Fig. 5, left panel.

Adding the delay and enterocyte compartments and increasing the FTC of β-carotene from the enterocyte compartment to the plasma chylomicron compartment produced an intermediate model that predicted the initial rise in plasma β-carotene-d_8 concentration very well. At the same time, this version of the model predicted a single peak with a shoulder (Fig. 5, left panel) for the plasma β-carotene-d_8 concentration–time curve instead of the two peaks indicated by the experimental observations. This discrepancy was resolved by increasing the FTC for β-carotene from the plasma chylomicron compartment to the liver β-carotene compartment (Fig. 5, right panel). The two β-carotene peaks were not resolved when this FTC was too small (see left panel).

While adjustments in model parameters (adding delay and enterocyte compartments and adjusting several FTCs) produced a model that predicted the initial rise and the two peaks in plasma β-carotene-d_8, it was still unable to match the decay portion of the second peak of plasma β-carotene-d_8 concentration–time curve, i.e., it was unable to sustain the observed concentration of plasma β-carotene-d_8 (see right panel of Fig. 5). Therefore, a second slower turnover liver β-carotene compartment was added

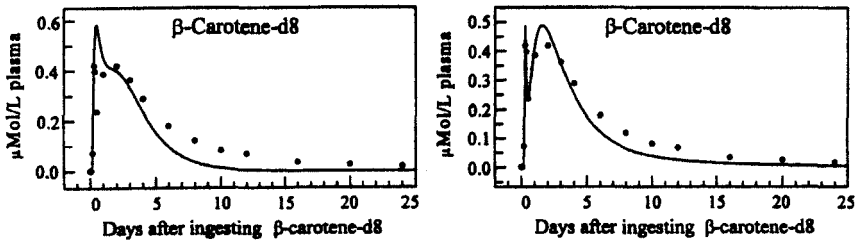

FIG. 5. Model prediction of the initial rise in plasma β-carotene after adding delay compartment (left panel) and the resolution of the plasma β-carotene peaks after adding an additional (enterocyte) compartment and adjusting several FTCs (right panel).

to the model which allowed the liver β-carotene to slowly flow into plasma (possibly via hepatic lipoprotein). Adding the second liver β-carotene compartment provided a slower decay rate for the plasma β-carotene-d_8 concentration–time curve and thus enabled the compartmental model to more accurately predict the plasma β-carotene-d_8 data (Fig. 4). Flow was calculated as the mass of analyte in the donor compartment multiplied by the FTC of the analyte from the donor to the recipient compartment.

Fitting the plasma retinoid-d_4 concentration–time curve was more challenging because the exact site of origin and identity (retinol-binding protein–retinol-d_4 from liver and/or retinyl-d_4 ester from enterocyte) of this β-carotene-d_8 metabolite was unclear. However, the time of the plasma peak, in between the first and second β-carotene-d_8 peaks, suggested three possible origins for retinoid-d_4.

First, the plasma retinoid-d_4 could have originated in the liver exclusively, thus representing RBP-ROH formed in and released slowly from the liver because the overall shape and the peak location of the plasma retinoid-d_4 concentration–time curve was very similar to that seen when the same subject had ingested retinyl-d_4 acetate in a previous experiment (Song *et al.*, 1995). Yet even if the observed retinoid-d_4 peak represented RBP-ROH exclusively from the liver, some portion of the plasma retinoid-d_4 still could have originated in the enterocyte, possibly as a polar retinoid-d_4 and have been transferred to the liver directly via portal blood without detection in the plasma. After all, it has already been shown that intestinally perfused [^{14}C]β-carotene is converted to polar retinoids that enter the liver via portal blood (Wang *et al.*, 1992) and that intraportally injected [^{14}C]retinoic acid (a retinoid metabolite of β-carotene) appears promptly in bile (Zackman *et al.*, 1966). It is also possible that a small retinyl-d_4 ester peak might have been missed entirely if it occurred between blood collection times. The last explanation is unlikely, however, due to the frequency of the blood collections.

Under the second theory, the plasma retinoid-d_4 could have originated in the enterocyte, thus representing retinyl-d_4 ester derived from β-carotene-d_8 there; that reaction could delay the timing (after ingesting β-carotene-d_8) of the plasma retinoid-d_4 peak. However, the width of plasma retinoid-d_4 peak spans several days, which far exceeds the expected duration of retinyl ester in the circulation. Although retinyl-d_4 ester was not specifically measured in the present study, in an ancillary study the same subject subsequently ingested 73 μmol nonlabeled β-carotene and retinyl ester was measured in whole plasma and in very low (VLDL), low (LDL), and high density lipoproteins (HDL) at 0, 7, 12, and 24 hr later. Because the subject ate foods devoid in vitamin A and carotenoids during the experiment,

it was assumed that the ingested β-carotene was the source of the low concentration of retinyl ester found in VLDL, LDL, HDL, and whole plasma. It was concluded that small amounts of retinyl ester were formed from β-carotene and/or that this metabolite of β-carotene was taken up by the liver extremely rapidly (Cortner *et al.*, 1987).

If conversion of β-carotene to retinyl ester in the enterocyte were small, it might be a rate-limiting step that could be augmented by hepatic conversion, since the liver also contains the carotenoid-15,15′-dioxygenase enzyme that catalyzes this process. To test if the compartmental model could predict such system behavior accurately if the liver were the only site for conversion, model parameters were altered so that only intact β-carotene-d_8 was absorbed and conversion to retinyl-d_4 ester in the enterocyte did not occur. Under these conditions, the compartmental model could not predict the experimental observations because fitting the first β-carotene-d_8 peak limited the amount of β-carotene-d_8 and retinoid-d_4 which was introduced into the system, and thus underestimated either the second β-carotene-d_8 peak or the retinoid-d_4 peak. It was concluded therefore, that the enterocyte is an important site of conversion of β-carotene to retinoid. Considerable evidence already exists for conversion of β-carotene to retinoid in the intestine (Dimitrov *et al.*, 1988; Olson, 1989; Wang *et al.*, 1992; Scita *et al.*, 1993).

Finally, we speculated that the plasma retinoid-d_4 could originate from both the enterocyte and the liver and thus represent a mix of retinol-d_4 and retinyl-d_4 ester; the latter would be removed from plasma very rapidly thereby keeping its concentration low. We had already determined in our examination of our first two theories that retinyl esters are cleared rapidly from plasma (Cortner *et al.*, 1987) and that the compartmental model could not predict the experimental observations when it was assumed that the plasma retinoid-d_4 originated from either the enterocyte or the liver alone. It became clear, therefore, that the retinoid-d_4 was a mix of retinyl-d_4 ester and retinol-d_4. Since retinyl-d_4 ester and retinol-d_4 (RBP-ROH) originate from the enterocyte and the liver, respectively, it was concluded that both organs play important and complementary roles in converting β-carotene to retinoid. It would be exceedingly interesting to discover if body reserves of retinol and/or β-carotene regulate conversion of β-carotene to retinoid at the enterocyte and/or the liver.

A second liver retinol (retinyl ester) compartment was added to the model for reasons analogous to those for adding a second liver β-carotene compartment. The experimental observations show an initial rise and fall in plasma retinol-d_4 concentration, then a sustained plasma retinol-d_4 level for ~16 days after ingesting β-carotene-d_8 (Fig. 4). Prior to adding the second liver retinol compartment, the model predicted that almost all

retinol-d_4 disappeared from the plasma within 24 days of ingesting β-carotene-d_8; this was not consistent with the sustained plasma retinol-d_4 concentrations seen experimentally. A second liver retinol (retinyl ester) compartment is consistent with existing knowledge that the histologically distinct hepatic parenchymal and stellate cells both contain retinyl ester. Stellate cells probably store retinol for the long term and turn it over more slowly (smaller FTC) than parenchymal cells. This phenomenon is the likely reason for the additional retinoid compartments in order for the model to predict the experimental observations.

V. STATISTICAL CONSIDERATIONS

Once the model provides a good fit of experimental observations, the statistical certainties of the model parameters are inspected. If parameters are highly correlated, it is often possible to alter one parameter and compensate for the alteration with another parameter without compromising the fit of model. For example, in the compartmental model of the dynamics of β-carotene metabolism, β-carotene absorption was highly (positively) correlated with the irreversible loss of β-carotene from the EHT compartment. Therefore, the absorption of β-carotene and its irreversible loss from the EHT could be increased simultaneously, along with minor adjustments to a few other FTCs, without materially altering the compartmental model's prediction of the experimental observations.

It must be realized, however, that the data used to build a particular compartmental model may not always provide sufficient statistical certainty of a given parameter's value. Because retinol-d_4 and retinyl-d_4 ester were not measured individually in the plasma after the subject ingested the β-carotene-d_8, we were unable to determine with statistical certainty the FTCs specifically for retinyl ester. Movement of retinyl ester from the enterocyte into the plasma was highly correlated with its removal from the plasma into the liver via chylomicron remnant. Therefore, the FTCs describing movement of retinyl ester from the enterocyte to the plasma and from the plasma to the liver could be increased simultaneously without compromising the model's prediction of the experimental observations.

When some of the model parameters lack sufficient statistical certainty, the investigator may search the scientific literature for relevant information and use it to set constraints on the numerical values of some parameters of the model. Several statistical constraints were added in constructing the model shown in Fig. 3. The FTC of retinyl ester from the chylomicron retinyl ester to the fast turnover liver retinyl ester compartment was constrained to be inside the range of two statistical deviations of 60 $\pm$ 36/day (mean $\pm$

SD) in order to correspond with the known half-life of chylomicron retinyl esters (15 ± 10 min) in healthy adult men (Cortner *et al.*, 1987). Also, the model intestinal absorption of β-carotene was constrained to be inside the range of two statistical deviations of 15 ± 4.5% based on a β-carotene balance study (Bowen *et al.*, 1993) in which 4.3 ± 0.8 μmol of a 28-μmol dose of β-carotene was absorbed in healthy subjects. Each of these constraints was achieved by including additional data points in the model. Finally, the irreversible loss of retinol from the model system was constrained to a minimum value of 0.7 μmol/day based on the rate of vitamin A depletion in humans (Sauberlich *et al.*, 1974). These additions to the model provided good statistical certainty on all model parameters, as the FSDs of the FTCs were <25% (see Table I).

The final version of the compartmental model shown in Fig. 1 was designed to predict the experimental observations and provide a good analogy of the system under investigation using a minimum number of compartments to favor simplicity and statistical certainty. Increasing the number of compartments can lead to a model whose parameters cannot be calculated with statistical certainty from the limited data (we did not have serial biopsies of liver, EHT, etc.), and this is usually reflected by numerical values with large FSDs. In general, when the FSD of a given model-calculated quantity is ≥~60% of the quantity, attempts are made to improve the statistical certainty of that quantity either by adding to the model more experimental observations related to the quantity (i.e., statistical constraints) or by removing compartments from the model (which reduces the number of quantities that must be calculated by the model). An intermediate version of the compartmental model of the dynamics of β-carotene metabolism had a series of liver β-carotene compartments aimed at providing a delay between the first and second peaks in the plasma β-carotene-d_8 data. However, because the FTCs of analyte among those liver compartments could not be obtained with statistical certainty from the limited data, the extra liver β-carotene compartments were replaced by one slow turnover liver β-carotene compartment in order to effect the resolution of the two plasma β-carotene-d_8 peaks. In this way the final compartmental model had a minimum number of compartments and thus favored simplicity and statistical certainty.

Because of the need to employ minimally invasive procedures in studies involving human subjects, compartments that can be experimentally observed are usually limited to diet, blood, urine, and feces, while compartments such as liver and EHT, etc., usually can be observed only under special circumstances. Compartmental models are ideally suited to human kinetic studies because unobservable compartments, especially those that exchange analyte with blood, can be included in the model, and masses

TABLE I

FRACTIONAL TRANSFER COEFFICIENTS AND FLOW RATES FROM DONOR TO RECIPIENT COMPARTMENTS FOR PHYSIOLOGIC MODEL OF β-CAROTENE METABOLISM

Donor compartment	Recipient compartment	FTC	FSD	Flow
Independent fractional transfer coefficients				
Gastrointestinal tract (GIT)	GIT delay	53.02	0.056	1.53
Enterocyte	Chylomicron β-carotene	7.98	0.055	1.24
Chylomicron β-carotene	Fast turnover liver β-carotene	34.76	0.059	1.24
Fast turnover liver β-carotene	Slow turnover liver β-carotene	0.076	0.20	0.337
Fast turnover liver β-carotene	Lipoprotein β-carotene	0.39	0.099	1.71
Slow turnover liver β-carotene	Lipoprotein β-carotene	0.11	0.16	0.337
Lipoprotein β-carotene	Fast turnover liver β-carotene	1.02	0.16	1.22
Lipoprotein β-carotene	Extra hepatic tissue β-carotene	0.70	0.092	0.835
Enterocyte	Chylomicron retinyl ester	1.91	0.11	0.297
Fast turnover liver β-carotene	Fast turnover liver retinyl ester	0.091	0.088	0.405
Fast turnover liver retinyl ester	Slow turnover liver retinyl ester	2.60	0.22	13.2
Fast turnover liver retinyl ester	Retinol-binding protein retinol	2.74	0.11	13.9
Slow turnover liver retinyl ester	Retinol-binding protein retinol	0.041	0.11	13.2
Retinol-binding protein retinol	Fast turnover liver retinyl ester	2.99	0.21	26.4
Extra hepatic tissue β-carotene	Irreversible loss β-carotene	0.088	0.083	0.835
Retinol-binding protein retinol	Irreversible loss retinol	0.079	0.059	0.702
Dependent fractional transfer coefficients				
GIT	Irreversible fecal loss of β-carotene	187.0	0.016	5.42
Chylomicron retinyl ester	Fast turnover liver retinyl ester	122.7	0.077	0.297
Fixed fractional transfer coefficient, time delay, subdivisions/delay compartment				
Delay time in hours		4.5		
Subdivisions of delay compartment		2.0		

Note: FTC is the fractional transfer coefficient; its units are per day. FSD is fractional standard deviation of FTC. Flow (rates) are μmol/day. Irreversible loss of β-carotene (fecal) = 240 − FTC from GIT to GIT delay compartment. FTC from chylomicron retinyl ester to fast turnover liver retinyl ester = 60 ± 36. Values apply to model in Figure 3. Reprinted with permission from Novotny *et al.* (1995).

and exchange of analyte can be proposed for them as hypotheses to be tested. In this way, a thoughtfully constructed compartmental model can extract considerable information concerning the dynamics of nutrient metabolism in humans using minimally invasive experimental procedures.

Finally, as indicated earlier, the test subject received a relatively large dose of β-carotene-d_8 (73 μmol). Despite the introduction of a large dose

of tracer, we had assumed that it would not affect the mechanisms present for metabolism of the tracee (the nonlabeled β-carotene). Metabolic processes of the tracee are indicated by the FTCs, and FTCs usually change when new mechanisms (pathways) are induced to metabolize the tracee. A compartmental model that predicted the behavior of the tracer, the tracee in the presence of the tracer, and the steady state of the system under investigation simultaneously, with the same set of FTCs, is consistent with the assumption that the large dose of tracer did not affect the mechanisms for metabolism of the tracee after absorption. We cannot state at this time if absorption of β-carotene is affected by the tracer dose or by physiologic state, gender, age, or nutritional status as only one subject was studied.

VI. THE FINAL MODEL

The resulting physiologic compartmental model of the dynamics of β-carotene metabolism in a human volunteer is shown in Fig. 3. The numbers in the compartments represent the model-predicted steady-state masses in μmol/compartment, and the numbers beside each arrow represent the flow rates in μmol/day (in the direction of the arrow) of analyte from donor to recipient compartments. Flow rate equals FTC from donor to recipient compartment multiplied by the mass of analyte in the donor compartment.

Figure 4 shows the compartmental model prediction of plasma β-carotene-d_8 and retinol-d_4 as a function of time after ingesting the β-carotene-d_8 (fitted lines) along with the experimentally observed data (filled circles) in the left panels. The right panels show the compartmental model prediction of plasma total β-carotene and total retinol as a function of time after ingesting the β-carotene-d_8 (fitted lines) along with the experimentally observed data (filled circles). The compartmental model's prediction of all four measurements was quite accurate (Fig. 4).

Table I summarizes the FTCs for β-carotene and retinol metabolism. Table I also summarizes the flow rates of β-carotene and retinoid from donor to recipient compartments during steady state. As the mass of analyte in the system changes, the flows will also change, but the FTCs are expected to remain constant unless alternate pathways (mechanisms) for metabolism of the tracee are induced by the large dose of tracer.

VII. SYSTEM BEHAVIOR PROPOSED BY THE MODEL

The model in Fig. 3 was proposed by adjusting the connectivity of the model to improve the fit to match the existing experimental observations,

and it was modified until it provided an adequate match. The model therefore represents the dynamics of β-carotene metabolism in an adult human as an hypothesis to be tested. Highlights of dynamics of β-carotene metabolism proposed by the physiologic compartmental model are summarized in Table II. The model results propose that 22% of the β-carotene dose was absorbed: 18% as intact β-carotene and 4% as retinoid derived from β-carotene. Of the total retinoid formed from ingested β-carotene, 57% was formed in the liver and 43% was formed in the intestine. The model also proposes that 33% of the β-carotene passing through the liver was converted to retinol.

The residence time for β-carotene in the test subject was predicted by the compartmental model to be 51 days. The residence time of 51 days is in excellent agreement with the 56-day mean sojourn time (MST = residence time) that can be calculated from the rate of decrease in plasma β-carotene concentration of women fed a diet of natural foods very low in carotene (Dixon *et al.*, 1994).

At the same time, the 51-day residence time for β-carotene is substantially longer than the 13-day MST predicted from the empirical polyexponential description of the experimental observations in our system under investigation (presented in Section IX of this paper). While the reason for this discrepancy between the MSTs predicted by the compartmental model and the empirical description calculated from the same experimental observa-

TABLE II

SELECTED RESULTS FROM PHYSIOLOGIC COMPARTMENTAL MODEL OF β-CAROTENE METABOLISM

Parameter	Value[a]
Portion of the β-carotene-d_8 dose that was absorbed	22%
Portion taken up as intact β-carotene-d_8	17.8%
Portion taken up as retinoid-d_4 derived from β-carotene-d_8	4.2%
Liver reserves of β-carotene	7.5 μmol
Liver reserves of retinol	324 μmol
Portion of retinoid formed from intestinal β-carotene conversion	43%
Portion of retinoid formed from liver β-carotene conversion	57%
Portion of liver β-carotene converted to retinoid	33%
Residence time of β-carotene in body	51 days
Residence time of retinol in body	474 days
Average intake of β-carotene by test subject from dietary sources	6.95 μmol/day (3.7 mg/day)

[a] Values apply to the compartmental model in Fig. 3. All values represent those predicted by the model in Fig. 3. Reprinted with permission from Novotny *et al.* (1995).

tions is unclear, it is likely that the empirical description underestimated the MSTs because sites for disposal and release of β-carotene are not limited to the accessible compartments (Cobelli and Saccomani, 1992). Also, the empirical description relies exclusively on plasma β-carotene concentration to determine MST and the kinetics of plasma β-carotene may not mimic those of tissue β-carotene. The compartmental model considers β-carotene present in liver and extrahepatic tissue (inaccessible compartments) as well as in plasma (an accessible compartment) in arriving at residence time.

The residence time for retinol in the test subject was predicted by the compartmental model to be 474 days. The residence time of 474 days is in excellent agreement with the 460 day MST that can be calculated from the data of Song *et al.* (1995) using the enrichment ratio method (Cobelli and Saccomani, 1992). Also, an MST of 105 to 337 days can be calculated from the half-life values (75 to 241 days) of body vitamin A reported by Sauberlich *et al.* (1974) who depleted human subjects with vitamin A-deficient diets. At the same time the empirical description predicted the MST for retinol to be 26 days. While the reason for such a large discrepancy in MST (474 versus 26 days) between the compartmental model and the empirical description prediction is unclear, it is not likely to be accounted for by slight errors in estimating the final slope of the plasma retinol-d_4 decay curve. Because the compartmental model embodies several features of retinol metabolism (*de novo* production and release of retinol can occur in unobservable compartments, etc.) in addition to plasma retinol concentrations, its predicted MST is more likely to better reflect the dynamics of retinol metabolism.

The compartmental model of β-carotene metabolism presented here is compatible with previously developed compartmental models of retinol metabolism (Green *et al.*, 1985; Lewis *et al.*, 1990). For example, the compartmental model of the dynamics of β-carotene metabolism features two kinetically distinct pools of retinol in the liver, recycling of plasma retinol by liver, and irreversible loss of retinol from the plasma. These aspects of retinol metabolism (predicted by the compartmental model) are compatible with already described aspects of retinol metabolism.

VIII. UNOBSERVABLE SYSTEM BEHAVIOR PROPOSED BY THE MODEL

In addition to the information presented in Table II, the physiologic compartmental model of the dynamics of β-carotene metabolism was constructed and used to also provide values for critical parameters so that

unobserved portions of the dynamics of the system under investigation could be predicted. The unobserved portions of the dynamics of β-carotene metabolism that were predicted include the masses of β-carotene and retinoid in plasma, liver, and EHT compartments, etc., as shown in Figs. 6 and 7. Some unobserved portions that were predicted are now discussed. β-Carotene-d_8 first appears (peaks) in the plasma when chylomicrons are expected to appear and then it disappears rapidly (Cortner *et al.*, 1987) into the fast turnover liver β-carotene-d_8 compartment. β-Carotene-d_8 reappears in the plasma as a broader peak that extends over several days consistent with the expectation that this is lipoprotein-associated β-carotene that undergoes considerable recycling between the plasma and the liver before it is finally removed from the plasma via a hepatic receptor mechanism and disposed of by the liver in bile.

The fast turnover liver β-carotene-d_8 curve exhibits a narrow peak after ingestion of the experimental dose, and it is similar to the predicted fast turnover liver retinoid-d_4 curve. The slow turnover liver β-carotene-d_8 peak is broader than the fast turnover liver β-carotene-d_8 peak and decays to near zero in approximately 50 days after ingestion of the labeled dose. Notice that the slow turnover liver β-carotene-d_8 level does not remain elevated as long as the slow turnover liver retinol-d_4. The slow turnover liver β-carotene decays in a fashion similar to the slow turnover liver β-carotene-d_8, as expected, since the β-carotene-d_8 is the source of the elevated slow turnover liver β-carotene.

Extrahepatic β-carotene-d_8 content and the extrahepatic total β-carotene content are predicted to disappear slowly, in agreement with the calculated MST of 51 days and in agreement with the observed skin-yellowing of individuals who ingest large amounts of β-carotene regularly. It is possible that the β-carotene present in extrahepatic tissues serves as a reserve of retinoid precursor as appears to happen in the corpus luteum. Also, the conversion of β-carotene to β-apocarotenals and retinoids has been demonstrated in lung, kidney, and adipose of human, monkey, ferret, and rat (Wang *et al.*, 1991). Finally, the uptake and cleavage of β-carotene by cultures of rat small intestine cells and by human lung fibroblasts has been demonstrated by Scita *et al.* (1993).

The predicted chylomicron retinyl-d_4 ester curve is characterized by a sharp peak similar to that of the β-carotene-d_8, again in accord with the expected rapid clearance of chylomicrons following a meal. The predicted plasma retinol-binding protein–retinol-d_4 curve shows an initial rise and fall, then a sustained level of retinol-d_4 after the β-carotene-d_8 dose. This is very similar in shape to that seen when the same subject ingested retinyl-d_4 acetate in a previous experiment (Song *et al.*, 1995). The sustained level of retinol-d_4 is a result of the slow release of retinoid into the plasma from

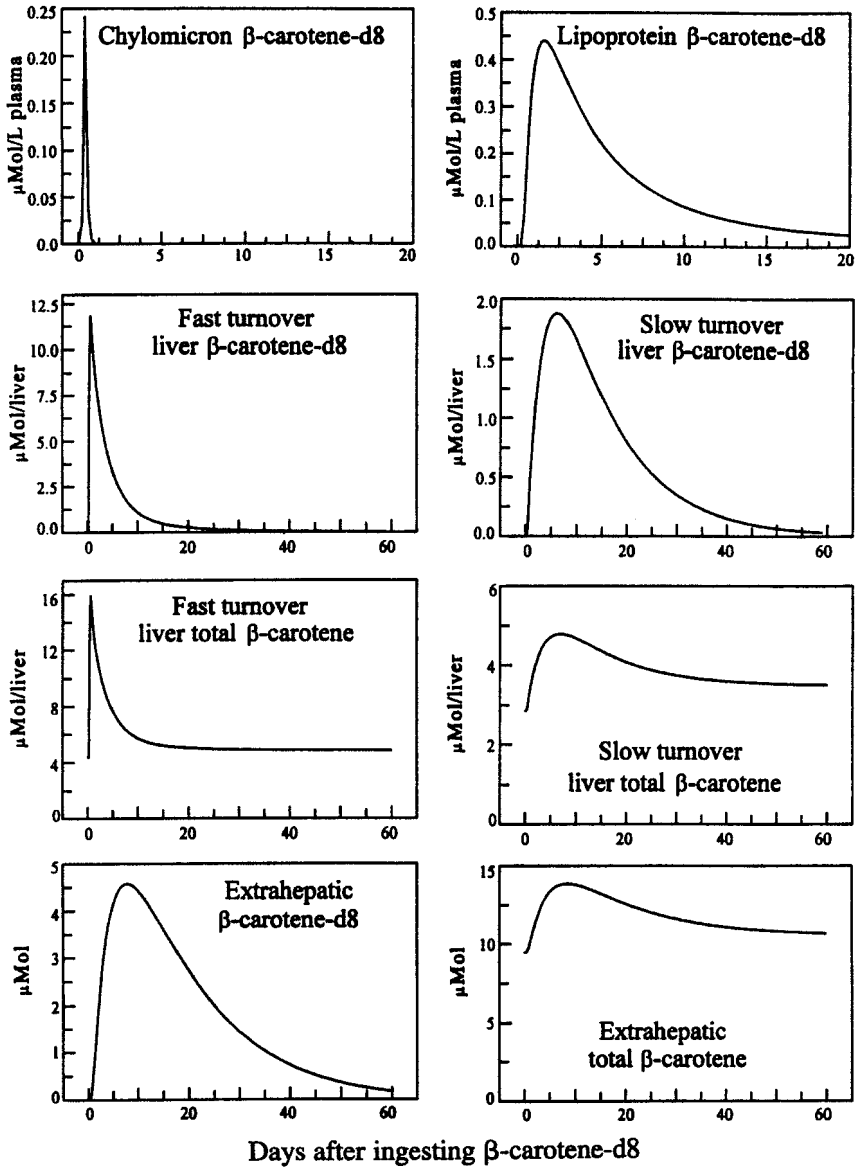

FIG. 6. Compartmental model predicted masses and concentrations of β-carotene in plasma, liver, and extrahepatic tissue of a healthy adult who ingested a single 73-μmol dose of β-carotene-d_8 orally. Panels labeled "Fast turnover liver total β-carotene," "Slow turnover liver total β-carotene," and "Extrahepatic total β-carotene" each include protio and deuterated species.

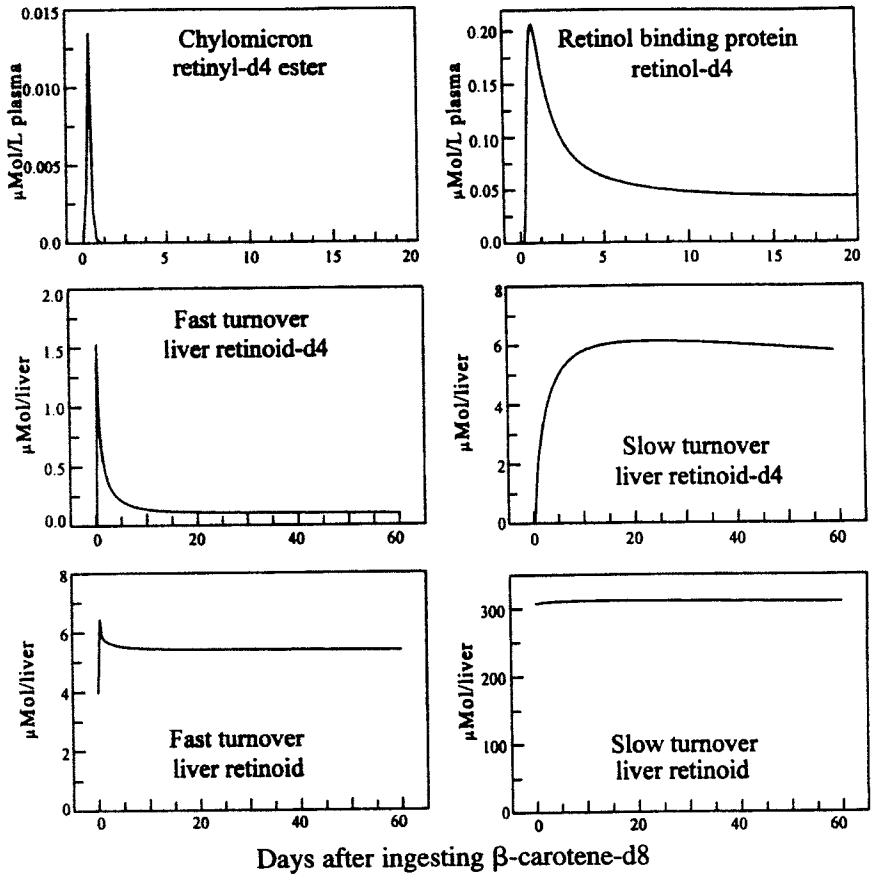

FIG. 7. Compartmental model predicted masses and concentrations of retinol and retinyl ester in plasma, liver, and extrahepatic tissue of a healthy adult who ingested a single 73-μmol dose of β-carotene-d_8 orally. The "Fast turnover liver retinoid" (bottom left) and "Slow turnover liver retinoid" (bottom right) each include the protio and deuterated species.

the slow turnover liver retinyl ester pool and the recycling of retinol by the liver.

The fast turnover liver retinoid-d_4 curve exhibits a narrow peak after the β-carotene-d_8 dose, while the slow turnover liver retinoid-d_4 peak rises and remains elevated. This indicates that the retinoid-d_4 is expected to have remained stored in the subject's liver for an extended time after ingesting the β-carotene-d_8. The slow turnover liver retinoid mass seems not to have been influenced by the ingested dose of the β-carotene-d_8. This is probably related to the abundant liver stores of vitamin A already present in this

experimental subject; the slow turnover liver vitamin A stores alone exceeded 300 μmol. The ~7 μmol total retinoid-d_4 formed from the 73-μmol dose of β-carotene-d_8 was very small in comparison to the subject's liver vitamin A stores. Such a dose of β-carotene might be anticipated to have a much greater influence on the slow turnover liver retinoid if the subject's total body reserve of vitamin A were minimal (i.e., liver stores $\leq$50 μmol). Future studies with subjects of varying vitamin A status will clarify the effect (ability) of β-carotene intake on (to replenish and/or sustain) tissue retinoid concentrations.

The compartmental model was also able to predict the efficiency of conversion of β-carotene to vitamin A in our subject. The model predicted that 1 μg dietary β-carotene yielded 0.054 μg retinol (the same as 0.101 μmol retinol/μmol β-carotene). The 0.054-μg value is considerably lower than the 0.167 μg retinol/μg β-carotene which is widely accepted. However, the 0.167-μg value was established in growing rats with low reserves of retinol who were adapted to maximizing the retinol yield (Brubacher and Weiser, 1985). If our subject had been in marginal or deficient vitamin A status, the predicted yield would probably have exceeded 0.054 μg retinol/μg β-carotene. Further studies are needed to determine the influence of vitamin A status on conversion of β-carotene to vitamin A and the ability of dietary carotene to maintain tissue retinoid.

Figures 6 and 7 and the preceding paragraphs exemplify the usefulness of modeling in predicting metabolite concentrations in tissues and biologic spaces that are difficult to observe experimentally. Once predictions have been made, the modeling process proceeds by testing these and other predictions and further modifying the model to fit with new experimental observations. In this way, the modeling process is open-ended as the model is continually refined as more and more experimental observations become available.

IX. EMPIRICAL DESCRIPTION OF THE EXPERIMENTAL OBSERVATIONS

To allow the information from the compartmental model of the dynamics of β-carotene metabolism to be compared with that from an empirical description of the same experimental observations, polyexponential fits (empirical descriptions) of our experimental observations were also made.

The plasma β-carotene-d_8 and retinol-d_4 concentration–time data were described using an empirical multiexponential description of the data using weighted, nonlinear least squares regression and the SAS NLIN procedure. Each observation was weighted by the reciprocal of its predicted value.

The plasma β-carotene-d_8 concentration–time curve was described by the five-term exponential equation $y(t) = -30.5e^{-12.3t} + 17.4e^{-5.7t} - 7.2e^{-3.3t} + 0.65e^{-0.27t} + 0.084e^{-0.067t}$. Figure 8 shows the observed plasma β-carotene-d_8 concentration–time data along with the concentration–time curve specified by the five-term exponential equation. The area under the concentration–time curve (AUC) was calculated as AUC = $\int_0^\infty y(t)dt$, and the area under the moment curve (AUMC) was calculated as AUMC = $\int_0^\infty t \times y(t)dt$. The AUC, AUMC, and AUMC/AUC for β-carotene-d_8 were calcu-

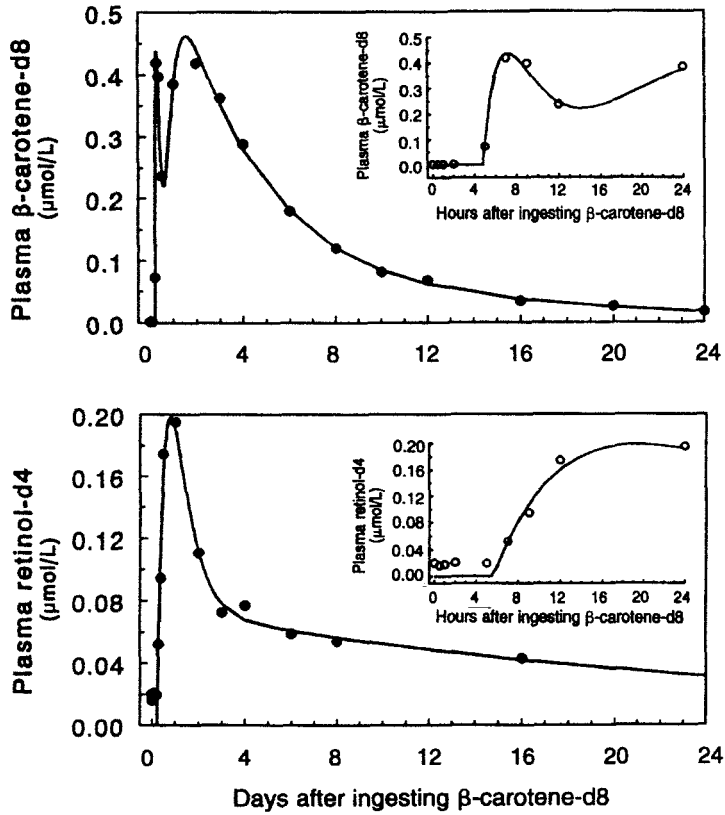

FIG. 8. Experimentally measured values (circles) and best-fit line using the empirical description of the concentrations of β-carotene-d_8 in plasma as a function of time after a 94-kg adult male ingested 73-μmol β-carotene-d_8 (top). Experimentally determined values (circles) and best-fit line using the empirical description of the concentrations of retinol-d_4 (derived from ingested β-carotene-d_8) by time after ingesting β-carotene-d_8 (bottom). Predicted values that were negative were set to equal zero. Reprinted with permission from Novotny *et al.* (1995).

lated to be 2.09 μmol × day/liter plasma, 27.31 μmol × day^2/liter plasma, and 13.05 days, respectively. The AUMC/AUC is commonly used to estimate the mean sojourn time (MST). The MST of β-carotene obtained with the empirical description is much shorter than that obtained with the compartmental model of the dynamics of β-carotene metabolism.

The plasma retinol-d_4 concentration–time data were described with the three-term exponential equation $y(t) = -1.338e^{-2.751t} + 0.883e^{-1.467t} + 0.07578e^{-0.03642t}$ using weighted, nonlinear least squares regression and the SAS NLIN procedure. Each observation was weighted and the AUC, AUMC, and MST were calculated as for plasma β-carotene-d_8. Figure 8 shows the concentration–time data along with the concentration curve specified by the three-term exponential equation for retinol-d_4. From this equation the AUC, AUMC, and MST for retinol-d_4 were calculated to be 2.20 μmol × day/liter plasma, 57.36 μmol × day^2/liter plasma, and 26.12 days, respectively. The MST of retinol obtained with the empirical description is much shorter than that obtained with the compartmental model of the dynamics of β-carotene metabolism.

The concentration–time curves generated with the empirical models both display nonzero y-intercepts. Because calculation of AUC and AUMC with a lower integration limit of $x = 0$ might introduce error into the values for AUC, AUMC, and MST, these parameters were also calculated by starting the integration at the x-intercept. When the integration limit was the x-intercept, the AUC, AUMC, and MST for β-carotene-d_8 were 3.17 μmol × day/liter plasma, 27.36 μmol × day^2/liter plasma, and 8.64 days, respectively. Under these conditions, the AUC, AUMC, and MST for retinol-d_4 were 2.23 μmol × day/liter plasma, 57.37 μmol × day^2/liter plasma, and 25.67 days, respectively. These results demonstrate that the error introduced into the AUC, AUMC, and MST values was small when the integration was performed from zero to infinity, and it was concluded that the discrepancy in residence time for β-carotene between the empirical description and the compartmental model was not due to the limits of integration.

X. FINAL ENCOURAGING WORDS

Modeling is an exciting and challenging means of investigating biological and physical systems. While the model presented here is specific for β-carotene, the general techniques and rationale used are typical of the compartmental modeling process. Many of the issues encountered in developing a compartmental model have been described in detail so that beginning modelers may have a greater understanding of how to proceed. We hope that our description of the development of the β-carotene model will pro-

vide a meaningful reference for the reader in future encounters with modeling, and we encourage the reader to embark on a modeling project of her/his own.

ACKNOWLEDGMENTS

The authors thank Meryl Wastney, Chris Calvert, Jan Peerson, and Peg Hardaway for reviewing the paper and Ali Arjomand for help in drawing some of the diagrams and figures. This research was supported by NIH (Grant RO1-DK-48307), USDA Regional Research (W-143), and Bridging Funds, Office of Vice Chancellor for Research at UCD.

REFERENCES

Abumrad, N. (1991). Mathematical models in experimental nutrition. *JPEN, J. Parenter. Enteral Nutr.* **15,** 44S–98S.

Bendich, A. (1993). Biological functions of dietary carotenoids. *Ann. N. Y. Acad. Sci.* **691,** 61–67.

Bergen, H. R. (1992). Synthesis of deuterated β-carotene. *In* "Methods in Enzymology" (L. Packer, ed.), Vol. 213, pp. 49–53. Academic Press, San Diego, CA.

Berman, M., and Weiss, M. F. (1978). "SAAM Manual," DHEW Publ. No. (NIH) 78–180. U.S. Govt. Printing Office, Washington, DC/National Institutes of Health, Bethesda, MD.

Bowen, P. E., Mobarhan, S., and Smith, J. C., Jr. (1993). Carotenoid absorption in humans. *In* "Methods in Enzymology" (L. Packer, ed.), Vol. 214, pp. 3–17. Academic Press, San Diego, CA.

Brubacher, G. B., and Weiser, H. (1985). The vitamin A activity of β-carotene. *Int. J. Vitam. Nutr. Res.* **55,** 5–15.

Clevidence, B. A., and Bieri, J. G. (1993). Association of carotenoids with human plasma lipoproteins. *In* "Methods in Enzymology" (L. Packer, ed.), Vol. 214, pp. 33–46. Academic Press, San Diego, CA.

Cobelli, C., and Saccomani, M. P. (1992). Accessible pool and system parameters: Assumptions and models. *JPEN, J. Parenter. Enteral Nutr.* **15,** 45S–50S.

Coburn, S. P. (1992). Application of models to the determination of nutrient requirements. *J. Nutr.* **122,** 687S–714S.

Cornwell, D. G., Kruger, F. A., and Robinson, H. B. (1962). Studies on the absorption of beta-carotene and the distribution of total carotenoid in human serum lipoproteins after oral administration. *J. Lipid Res.* **3,** 65–70.

Cortner, J. A., Coates, P. M., Le, N. A., Cryer, D. R., Ragni, M. C., Faulkner, A., and Langer, T. (1987). Kinetics of chylomicron remnant clearance in normal and in hyperlipoproteinemic subjects. *J. Lipid Res.* **28,** 195–206.

Dimitrov, N. V., Meyer, C., Ullrey, D. E., Chenoweth, W., Michelakis, A., Malone, W., Boone, C., and Fink, G. (1988). Bioavailability of β-carotene in humans. *Am. J. Clin. Nutr.* **48,** 298–304.

Dixon, Z. R., Burri, B. J., Clifford, A. J., Frankel, E. N., Schneeman, B. O., Parks, E., Keim, N. L., Barbieri, T., Wu, M. M., Fong, A. K. H., Kretsch, M. J., Sowell, A. L., and Erdman, J. W., Jr. (1994). Effects of a carotene-deficient diet on measures of oxidative susceptibility and superoxide dismutase activity in adult women. *Free Radicals Biol. Med.* **17,** 537–544.

Dueker, S. R., Lunetta, J. M., Jones, A. D., and Clifford, A. J. (1993). Solid-phase extraction protocol for isolating retinol-d_4 and retinol from plasma for parallel processing for epidemiologic studies. *Clin. Chem. (Winston-Salem, N.C.)* **39,** 2318–2322.

Dueker, S. R., Jones, A. D., and Clifford, A. J. (1994). Stable isotope methods for the study of β-carotene-d_8 metabolism in humans utilizing tandem mass spectrometry and high performance liquid chromatography. *Anal. Chem.* **66,** 4177–4185.

Goodman, D. S., and Huang, H. S. (1965). Biosynthesis of vitamin A with rat intestinal enzymes. *Science* **149,** 879–880.

Green, M. H., and Green, J. B. (1994). Dynamics and control of plasma retinol. *In* "Vitamin A in Health and Disease" (R. Blumhoff, ed.), pp. 119–133. Dekker, New York.

Green, M. H., Uhl, L., and Green, J. B. (1985). A multicompartmental model of vitamin A kinetics in rats with marginal liver vitamin A stores. *J. Lipid Res.* **26,** 806–818.

Handelman, G. L., Haskell, M. J., Jones, A. D., and Clifford, A. J. (1993). Improved GC/MS determination of d4-retinol/retinol in human plasma. *Anal. Chem.* **65,** 2024–2028.

Krinsky, N. I. (1989). Carotenoids and cancer in animal models. *J. Nutr.* **119,** 123–126.

Krinsky, N. I., Cornwell, D. G., and Oncley, J. L. (1958). The transport of vitamin A and carotenoids in human plasma. *Arch. Biochem. Biophys.* **73,** 233–246.

Krinsky, N. I., Wang, X.-D., Tang, G., and Russell, R. M. (1994). Mechanism of carotenoid cleavage to retinoids. *Ann. N. Y. Acad. Sci.* **691,** 167–176.

Langer, T., Strober, W., and Levy, R. I. (1972). The metabolism of low density lipoprotein in familial type II hyperlipoproteinemia. *J. Clin. Invest.* **51,** 1528–1536.

Lewis, K. C., Green, M. H., Green, J. B., and Zech, L. A. (1990). Retinol metabolism in rats with low vitamin A status: A compartmental model. *J. Lipid Res.* **31,** 1535–1548.

Novotny, J. A., Dueker, S. R., Zech, L. A., and Clifford, A. J. (1995). Compartmental analysis of the dynamics of β-carotene metabolism in an adult volunteer. *J. Lipid Res.* **36,** 1825–1838.

Olson, J. A. (1989). Provitamin A function of carotenoids: The conversion of β-carotene into vitamin A. *J. Nutr.* **119,** 105–108.

Olson, J. A., and Hayaishi, O. (1965). The enzymatic cleavage of beta-carotene into vitamin A by soluble enzymes of rat liver and intestine. *Proc. Natl. Acad. Sci. U.S.A.* **54,** 1364–1369.

Olson, R. E. (1992). Vitamins and carcinogenesis: An overview. *In* "Proc. First International Congress on Vitamins and Biofactors in Life Science in Kobe, 1991" (T. Kobayashi, ed.), pp 313–316. Center for Acad. Publications Japan. Tokyo, Japan.

Sauberlich, H. E., Hodges, R. E., Wallace, D. L., Kolder, H., Canham, J. E., Hood, J., Raica, N., Jr., and Lowry, L. K. (1974). Vitamin A metabolism and requirements in the human studied with the use of labeled retinol. *Vitam. Horm. (N. Y.)* **32,** 251–275.

Schmitz, H. H., Poor, C. L., Wellman, R. B., and Erdman, J. W., Jr. (1991). Concentrations of selected carotenoids and vitamin A in human liver, kidney and lung tissue. *J. Nutr.* **121,** 1613–1621.

Schmitz, H. H., Poor, C. L., Gugger, E. T., and Erdman, J. W. Jr. (1993). Analysis of carotenoids in human and animal tissues. *In* "Methods in Enzymology" (L. Packer, ed.), Vol. 214, pp. 102–116.

Scita, G., Aponte, G. W., and Wolf, G. (1993). Uptake and cleavage of β-carotene by cultures of rat small intestinal cells and human lung fibroblasts. *In* "Methods in Enzymology" (L. Packer, ed.), Vol. 214, pp. 21–32. Academic Press, San Diego, CA.

Snyder, W. S., Cook, M. J., Nasset, E. S., Karhausen, L. R., Howells, G. P., and Tipton, I. H. (1975). "Report of the Task Group on Reference Man," Int. Comm. Radiol. Prot. No. 23, pp. 273–334. Pergamon, New York.

Song, K. S., Muller, H. G., Clifford, A. J., Furr, H. C., and Olson, J. A. (1995). Estimating derivatives of pharmacokinetic response curves with varying bandwidths. *Biometrics* **51,** 12–20.

van Vliet, T., van Scheik, F., and van den Berg, H. (1992). β-Carotene metabolism: The enzymatic cleavage to retinal. *Neth. J. Nutr.* **53,** 186–190.

Wang, X.-D., Tang, G. W., Fox, J. G., Krinsky, N. I., and Russell, R. M. (1991). Enzymatic conversion of β-carotene into apo β-apo-carotenals and retinoids by human, monkey, ferret, and rat tissues. *Arch. Biochem. Biophys.* **285,** 8–16.

Wang, X.-D., Krinsky, N. I., Marini, R. P., Tang, G., Yu, J., Hurley, R., Fox, J. G., and Russell, R. M. (1992). Intestinal uptake and lymphatic absorption of β-carotene in ferrets: A model for human β-carotene metabolism. *Am. J. Physiol.* **263,** G480–G486.

Zackman, R. D., Dunagin, P. E., and Olson, J. A. (1966). Formation and enterohepatic circulation of metabolites of retinol and retinoic acid in bile duct-canulated rats. *J. Lipid Res.* **7,** 3–9.

Zulim, R. A., Lunetta, J. M., Corso, F. A., Dueker, S. R., Schneider, P. D., Joyce, V., Rippon, M. B., Wolfe, B. M., and Clifford, A. J. (1995). Retinol and β-carotene concentrations in tissues of patients with and without breast or colon cancer. *Cancer* (*Philadelphia*) (submitted for publication).